Motion of Three Vortices near Collapse

X. Leoncini[1], L. Kuznetsov[2]*, and G. M. Zaslavsky[1,2]

August 31, 1999

[1]Courant Institute of Mathematical Sciences, New York University, 251 Mercer St., New York, NY 10012, USA

[2]Department of Physics, New York University, 2-4 Washington Place, New York, NY 10003, USA

Abstract

A system of three point vortices in an unbounded plane has a special family of self-similarly contracting or expanding solutions: during the motion, vortex triangle remains similar to the original one, while its area decreases (grows) at a constant rate. A contracting configuration brings three vortices to a single point in a finite time; this phenomenon is known as vortex collapse and is of principal importance for many-vortex systems. The self-similar motion (contracting or expanding) is

*Current adress: Division of Applied Mathematics, Brown University, Providence, RI 02912

not generic, it arises when vortex strengths and initial positions satisfy two special collapse conditions. Dynamics of close-to-collapse vortex configurations depends on the way the collapse conditions are violated. We show, that when two of the vortices are identical, it is possible to reduce a three-vortex system to a problem of motion of a particle in an effective potential, defined by initial conditions. Using the effective potential representation, a detailed quantitative analysis of different types of near-collapse dynamics is performed. We discuss time and length scales, emerging in the problem, and their behavior as the initial vortex triangle is approaching to an exact collapse configuration. Special features of passive particle mixing by a near-collapse flows are illustrated numerically.

1 Introduction

The importance of point vortex systems in applications is due to the dominant role of coherent vortical structures in many 2D turbulent flows. Experimental and numerical studies performed in [1]-[8] have demonstrated, that in cases of driven or freely decaying 2D turbulence a number of concentrated vortices develops out of an originally unstructured flow. In many situations, dynamics of this finite-size vortices can be reasonably well approximated by point-vortex models [9]-[11].

The number of vortices in a flow can be quite large, in which case a complete dynamical description gets intractable, but still can yield some impor-

tant statistical quantities [12, 13]. On the other hand, few-vortex systems can be investigated in much more detail. Recent interest in this area was mainly directed towards the study of Lagrangian chaos in different settings [14]-[19]. Apart from this, low-dimensional vortex dynamics is essential to understand the evolution of many-vortex flows, since it describes their "elementary interactions" [20]. Analysis of rare gas of vortex patches, performed in [21] indicates, that in the limit of low vortex density (vortex occupation less than one-two percent), strong interactions occur only between three vortices in a specific way, similar to the *three point-vortex collapse*. These processes may be thought of as resonance interactions in the vortex gas.

The phenomenon of finite-time collapse of three point vortices into one was studied by several authors [20, 22, 23, 24, 25]. For the collapse to happen certain conditions on vortex strengths and initial positions have to be satisfied exactly, so that in a real system, probability of this event is zero: true resonances do not occur. However, actual vortices have some characteristic size, and when distance between them gets comparable with their size, vortices experience a considerable distortion, and may merge together, which means, that from a broader physical point of view, a collapse can be thought of as a process which brings vortices close enough (up to their size) to each other. For three initially well-separated vortices to collapse in the above sense, their strength and positions may satisfy "resonance conditions" only approximately. We refer to this kind of motion as near-collapse dynamics. Its importance stems from the fact, that inter-vortex distances are changed

considerably (by orders of magnitude) during the motion, which brings the system to a different length-scale, where new physical mechanisms enter into play.

The dynamics of exact collapse is relatively simple due to a self-similarity of vortex motion in this case: a triangle formed by vortices (vortex triangle) rotates and shrinks, but stays similar to the initial one. Vortex triangle area decreases linearly with time, at a rate determined by vortex strengths and triangle shape [20]. A spatial reflection of a vortex triangle is equivalent to a time reversal, so that a reflection of a collapse configuration will experience an infinite self-similar expansion with the same rate of change of triangle area.

In this paper we perform a detailed analysis of near-collapse situations, when resonance initial conditions are slightly distorted, and/or vortex strengths are not precisely tuned. We restrict our attention to the case when two of the vortices are identical, for which it is possible to map the dynamics of vortex separation to a motion of a particle in a one dimensional potential. In section 2 the basic equations of vortex motion, their symmetries and corresponding first integrals are specified. Effective Hamiltonian for a three-vortex system with two identical vortices is introduced in section 3; using which different types of near-collapse dynamics are classified and analyzed. In section 4 we discuss various routes to collapse, i.e. the manner in which near-collapse motion types approach self-similarly contracting (expanding) solutions as initial configuration is taken closer to the exact resonance. In section 5 we give

a brief illustration of how the approach to collapse affects passive particle advection.

2 Dynamical equations

Point vortices are solutions of two-dimensional physical systems described by a conservation equation which is a generalization of the vorticity Euler equation. The dynamics of generalized vorticity Ω is given by:

$$\frac{\partial \Omega}{\partial t} + [\Omega, \psi] = 0 \,, \tag{1}$$

where $[\cdot, \cdot]$ is the usual Poisson bracket, and ψ is the stream function; an actual relation $\Omega = F(\psi)$ depends on a particular physical system; in case of Euler equation: $\Omega = -\nabla^2 \psi$. Equation (1) expresses the conservation of generalized vorticity along the path lines of the flow.

Point vortices are exact solutions of Euler equation (see for example [26]); they also are exact solutions in a more general case (1), when $\Omega = -\nabla^2 \psi + \psi / l_s^2$ where ψ, in this context, is related to the electric potential (in suitable units) in plasma, and l_s is a hybrid Larmor radius, a characteristic length which introduces a finite range interaction between concentrated vortices. In this case the usual logarithmic vortex pair interaction is replaced by a modified Bessel function K_0 interaction.

A point vortex system is defined by a vorticity distribution given by a

superposition of Dirac functions:

$$\Omega(\mathbf{x},t) = \sum_{i=1}^{N} k_i \delta\left(\mathbf{x} - \mathbf{x}_i(t)\right) \ , \tag{2}$$

where $\mathbf{x}$ is a vector in the plane of the flow, k_i is the circulation of i-th vortex, N is the total number of vortices, and $\mathbf{x}_i(t)$ is the vortex position at time t. Using this expression for the vorticity, and solving Poisson equation, in the Euler case, or Helmholtz equation, in the more general case, one obtains a stream function of a point vortex system. By Helmholtz theorem [27], the motion of vortices is determined by the value of the velocity field at the position of the vortex. If the velocity field is written as $\mathbf{v} = \mathbf{e}_z \wedge \nabla\psi + \nabla\phi$, where $\mathbf{e}_z$ is the unit vector perpendicular to the plane of the flow, and ϕ takes into account the potential flow, the equation of a point vortex motion is:

$$k_i \frac{d\mathbf{x}_i}{dt} = \mathbf{e}_z \wedge \frac{\partial H}{\partial \mathbf{x}_i} + k_i \nabla\phi \, . \tag{3}$$

where the Hamiltonian H, in case of an unbounded flow plane, is given by:

$$H = \frac{1}{2\pi} \sum_{i>j} k_i k_j U(|\mathbf{x}_i - \mathbf{x}_j|) \tag{4}$$

with the interaction potential $U(x) = -\log(x)$ in the Euler case, and $U(x) = \mathrm{K}_0(x)$ in the more general case (when $l_s \to \infty$ the modified Bessel function $\mathrm{K}_0(x)$ tends to $\ln(x)$). The Hamiltonian (4) is invariant under translation and rotation, which implies both the conservation of the two components of

vortex momentum:

$$Q \equiv \sum_{i=1}^{N} k_i x_i(t) = const. \qquad P \equiv \sum_{i=1}^{N} k_i y_i(t) = const. \tag{5}$$

and vortex angular momentum $K\mathbf{e}_z$ with:

$$K \equiv \sum_{i=1}^{N} k_i (x_i^2(t) + y_i^2(t)) = const. \tag{6}$$

When the distance between the vortices is smaller than the typical interaction length (l_s) the behavior of the two systems is similar ($\mathrm{K}_0(x) \sim \ln(x)$), in the opposite case, the energy decreases exponentially and the interactions between the vortices can be neglected. In the following, analytical computations will be made using the logarithmic interaction, which corresponds to the Euler flow, and we can expect the results to be qualitatively valid for the Bessel interaction as long as the vortices are not "too far" from each other.

Integrability of a point vortex system depends primarily on two things: the number of vortices N, and the shape of the domain D, occupied by the fluid [22, 28, 16]. For each domain shape, there exists a critical number N_{max}, such that motion of N_{max} vortices in D is integrable no matter what vortex strengths and positions are, and for some combination of $N_{max}+1$ vortices their motion is chaotic. Critical number depends on the symmetry of the fluid domain. On an unbounded plane three-point-vortex system is always integrable, and motion of four vortices is in general chaotic, so that $N_{max}(\mathbf{R}^2) = 3$. For less symmetrical domains N_{max} decreases, because of the

absence of corresponding first integrals, e.g. for a half-plane and for a circular domain $N_{max} = 2$, due to the absence of translational/rotational symmetry.

In this paper we consider a case of three vortices in an unbounded domain. We restrict our attention to the relative motion of vortices, taking inter-vortex distances R_i as prime variables. The notation we use is illustrated in Fig. 1. The invariance of the Hamiltonian (4) under translations allows us a free choice of the coordinate origin, which we put to the center of vorticity (when it exists). Then, the other two constants of motion (energy and angular momentum) written in a frame independent form become:

$$\begin{cases} H = -\frac{1}{2\pi}\left[k_1 k_2 \ln R_3 + k_1 k_3 \ln R_2 + k_3 k_2 \ln R_1\right] \\ K = k_1 k_2 R_3^2 + k_1 k_3 R_2^2 + k_3 k_2 R_1^2 \, . \end{cases} \tag{7}$$

The equations of motion 3 in the absence of potential flow ($\phi = const.$) yield the following non canonical system for the dynamics of the inter-vortex distances:

$$\begin{cases} k_1^{-1} R_1 \dot{R}_1 = A/\pi (R_2^{-2} - R_3^{-2}) \\ k_2^{-1} R_2 \dot{R}_2 = A/\pi (R_3^{-2} - R_1^{-2}) \\ k_3^{-1} R_3 \dot{R}_3 = A/\pi (R_1^{-2} - R_2^{-2}) \, , \end{cases} \tag{8}$$

where A is the area of the triangle $A_1 A_2 A_3$ (see Fig. 1), and $\dot{x}$ refers to the time derivative of x.

The physical system being defined, we shall now focus on the near collapse configuration. As mentioned earlier, for the three point vortex problem,

under certain conditions, which depends both on the initial conditions, and the vortex strengths, the motion is self similar, leading either to the collapse of the three vortices in a finite time, or by time reversal, to an infinite expansion of the triangle formed by the vortices. These conditions of a collapse or an infinite expansion of the three point vortices are:

$$K = 0 \tag{9}$$

$$\sum_i \frac{1}{k_i} = 0 \,, \tag{10}$$

i.e, the harmonic mean of the vortex strengths (10) and the total angular momentum in its frame free form (9), are both zero. Near a collapse configuration, the two conditions (9), (10) allow two different ways to approach the singularity. Namely, we can change initial conditions which changes the value of K, or change the vortex strength and modify the harmonic mean. Unfortunately the motion of the three vortices even though integrable is not easily computed analytically. It then seemed useful to restrict the problem to some less general case, assuming that the basic mechanisms of collapse should not differ much in the general case. To emphasize this last statement, let us first consider a general collapse situation, for which the total strength is k_{tot}. The following conditions are then fulfilled

$$\sum_i k_i = k_{tot} \,, \sum_i \frac{1}{k_i} = 0 \,, \tag{11}$$

which are equivalent to

$$\sum_i k_i = k_{tot}\,, \sum_i k_i^2 = {k_{tot}}^2\,. \tag{12}$$

The values for the vortex strengths corresponding to a collapse configuration are therefore located on the circle resulting from the intersection of the sphere of radius ${k_{tot}}^2$ and the plane imposing a total vortex strength equal to k_{tot}. Since we have a circle, we shall assume that, from this point of view, no special configuration exists, and any should be sufficient to describe qualitatively the different possible behaviors.

In the following we will be considering the case, when two of the three vortices are identical. Since the rescaling of time scales leads to a freedom in vortex strength normalization, we will assume

$$k_2 = k_3 = 1 \tag{13}$$

Then, in order for a collapse to happen, the strength of the third vortex has to satisfy (10) which gives the resonance value of the first vortex: $k_{1c} = -1/2$. We will be mostly interested in the situations, when k_1 is negative and close to its resonance value, so we will denote

$$k \equiv |k_1|\,, \tag{14}$$

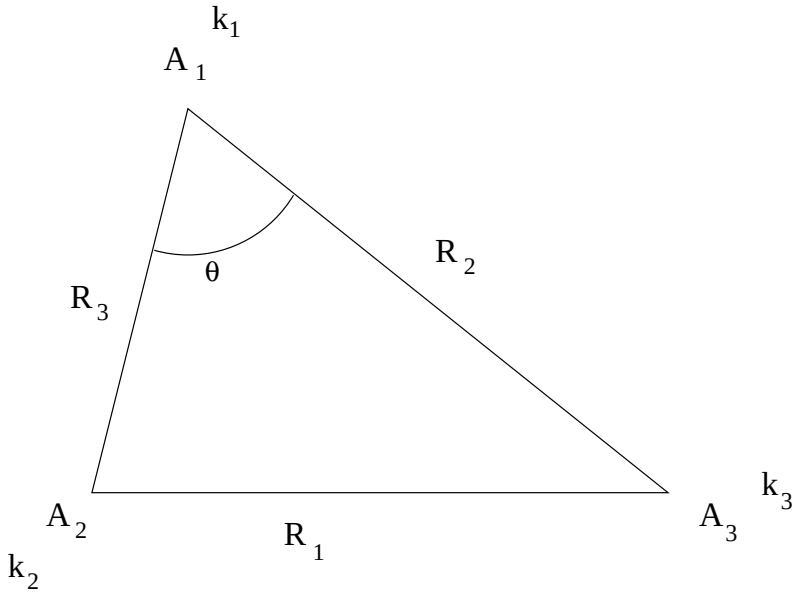

Figure 1: Notation chosen for the problem

and define the deviation from the resonance as

$$\delta = 1/2 - k\,. \tag{15}$$

3 Near-collapse dynamics of vortices

In the case when two out of three vortices are identical, there exists a convenient representation of the system dynamics in terms of a motion of a particle in a one-dimensional potential, parametrically depending on vortex initial condition. To derive this representation, we introduce a new set of variables: $X = R_1^2$, $Y = R_2^2 R_3^2$, and $Z = R_2^2 + R_3^2$. The constants of motion

(7) can be written as:

$$\begin{cases} \Lambda = e^{4\pi H} = Y^k/X \\ K = X - kZ\,. \end{cases} \tag{16}$$

where new parameter Λ is introduced instead of H in order to simplify formulas.

An equation on X can be directly obtained from the first equation of (8), squaring it gives:

$$\dot{X}^2 = 16A^2k^2\frac{(R_2^2+R_3^2)^2 - 4R_2^2R_3^2}{R_2^4R_3^4} = 16A^2k^2\frac{Z^2-4Y}{Y^2}\,. \tag{17}$$

Square of the vortex triangle area A can be found from geometrical identities

$$\begin{cases} A = \sqrt{Y}|\sin\theta|/2 \\ X = Z - 2\sqrt{Y}\cos\theta\,, \end{cases} \tag{18}$$

which leads to

$$16A^2 = 4Y - (X-Z)^2\,. \tag{19}$$

Using the expression for the constants of motion (16), we obtain:

$$\dot{X}^2 = \frac{[4k^2Y - (K-(1-k)X)^2][(K-X)^2 - 4k^2Y]}{k^2Y^2}, \tag{20}$$

where $Y = (\Lambda X)^{1/k}$. This equation has a form of an energy conservation law for a particle of mass 1 and zero total energy moving in a potential

$V(X;\Lambda,K,k)$, defined by

$$V(X;\Lambda,K,k) \equiv \frac{[(K-(1-k)X)^2-4k^2Y][(X-K)^2-4k^2Y]\}}{2k^2Y^2}\,. \qquad (21)$$

Indeed, equation (20) can be rewritten as

$$H_{eff}(\dot{X},X;\Lambda,K,k) \equiv P^2/2 + V(X;\Lambda\,K,k) = 0\,, \qquad (22)$$

with Hamiltonian equations

$$\dot{X} = \partial H_{eff}/\partial P \equiv P\,, \qquad \dot{P} = -\partial H_{eff}/\partial X\,. \qquad (23)$$

Thus, dynamics of vortex configuration is governed by an effective Hamiltonian H_{eff}, where the shape of the potential well V depends on the initial vortex positions through the values of first integrals Λ and K (16), and the strength of the first vortex k.

Effective Hamiltonian representation (22), gives a number of advantages, allowing to use simple standard techniques for one-dimensional conservative systems to find dynamical properties of vortex motion. In a sense, the problem is reduced to determining the shape of the potential V as a function of its parameters.

Before proceeding to the analysis of the types of potentials, emerging in our problem, we have to mention the restrictions, imposed on the system by the fact that three vortices form a triangle. Since this was not taken

into account in the derivation of the effective Hamiltonian (22), it may put additional boundaries on the possible values of X. Note, that since the effective energy H_{eff} in (22) is always zero, a motion exists only on the segments where the potential is negative. Therefore, triangle inequalities and the condition $V \leq 0$ define the physical domain of X. Triangle inequalities

$$|R_2 - R_3| \leq R_1 \leq R_2 + R_3 \,, \tag{24}$$

written in terms of new variables can be obtained by taking the square of (24): $Z - 2\sqrt{Y} \leq X \leq Z + 2\sqrt{Y}$, which is equivalent to

$$(X(k-1) + K)^2 - 4k^2 Y \leq 0 \,. \tag{25}$$

The condition (25) is equivalent to the positiveness of the right hand side of equation (19) and translates that the square of the area of the triangle $A_1A_2A_3$ is positive. The condition $V(X) \leq 0$ together with the triangle inequalities (25) imposes then

$$(K - X)^2 - 4k^2 Y \geq 0 \,, \tag{26}$$

Recalling that $Z > 0$, we have $X \geq K$, which together with inequality (26), gives finally

$$X \geq K + 2k\sqrt{Y} \,. \tag{27}$$

Now we have a precise information on where the motion should lie, and can proceed to the study of different regimes of near-collapse dynamics. Although the effective potential representation is valid for any $k \neq 0$, we will restrict our study (and our definition of "near-collapse") to the interval $k \in]0;1[$, since the special cases $k = 1$ (escaping vortex pair) and $k = 2$ (neutral tripole), as well as the degenerate case $k = 0$ (two vortices and a passive particle) bring up their specific singularities, unrelated to the collapse phenomenon. Let us consider different regimes such that each regime corresponds to a class of qualitatively similar motions [20]. Using the effective Hamiltonian representation (22), we infer that different regimes may be encountered corresponding to the number of roots of the potential $V(X;\Lambda,K,k)$ lying within the physical domain. This number changes with variation of the parameters (Λ, K, k).

Note, that the absolute value of K depends on the length units and can be scaled out of the problem. Indeed, the potential V and the physical domain boundary (27) are invariant under the scaling transformation (compare to (16))

$$X \to \frac{X}{|K|}, \qquad \Lambda \to \Lambda |K|^{\delta} , \tag{28}$$

and the problem can be reduced to the study of the three following cases

$$K = 1 \, , \; K = -1 \, , \; K = 0 \, , \tag{29}$$

where the last case is singular. In the following most of the figures illustrating

the problem will correspond to the values (29), although we will keep K as a scale parameter in formulas, keeping in mind, that only its sign is relevant to distinguish different regimes. Note that the scaling of Λ in (28), which can be rewritten in terms of vortex energy (7) as

$$H \to H + \delta \ln |K| \,, \tag{30}$$

leaves Λ and H unchanged, when $\delta = 0$, i.e. when vortex strengths exactly satisfy the collapse condition (10). The scales of the motion are determined by the value of the angular momentum K, while from a pure energetic point of view the motion would be thought as scale invariant.

3.1 Critical situations for $K \neq 0$

To detect bifurcations, leading to the appearance of new roots of the potential, we look for the degenerate roots of (21). As a first step, we just want to find these roots, leaving their detailed interpretation for the following paragraphs. Such roots X_c exist only for certain critical values Λ_c of the energy parameter Λ, and can be found from:

$$\begin{cases} V(X_c, \Lambda_c) = 0 \\ \partial V / \partial X (X_c, \Lambda_c) = 0 \end{cases} \tag{31}$$

The above system can be easily solved if one notices, that the potential (21) is written in a factorized form: $V = V_1 * V_2/(2k^2Y^2)$, with

$$V_1 \equiv [(K-(1-k)X)^2 - 4k^2Y], \qquad V_2 \equiv [(K-X)^2 - 4k^2Y] \tag{32}$$

Then, if a solution $X_c,\ \Lambda_c$ exists and is different from $X = 0$, it should be either a double zero of V_1 or V_2, or a zero of both V_1 and V_2.

We start from finding a double zero of V_2, which yields a system similar to (31), where V is substituted by V_2, that leads to:

$$\begin{cases} (X-K)^2 - 4k^2Y = 0 \\ 2kX\,(X-K) - 4k^2Y = 0 \end{cases} \tag{33}$$

and after some substitutions we readily obtain,

$$\begin{cases} X_{c_1} = K/2\delta \\ \Lambda_{c_1} = (K/2\delta)^{-2\delta} \end{cases} \tag{34}$$

For X_{c_1} to be positive, K and δ must have the same sign, so this bifurcation pertains to the physical region only for the cases $K > 0,\ k < 1/2$ and $K < 0,\ k > 1/2$ (it is easy to check that substitution of (34) into (27) turns the latter into an identity). Another solution, $X = K,\ \Lambda = 0$, corresponds to the situation when the negative vortex merges with one of the two others, reducing the system to a two-vortex case. Notice that X_{c_1} diverge as vortex strength collapse condition (10) is approached ($\delta \to 0, k \to 1/2$), which

announces a special behavior of the case $\delta = 0$, requiring a special treatment.

Double zeros of V_1 are found in the same manner. After some algebra we obtain:

$$\begin{cases} X_{c_2} = X_{c_1}/\left(1-k\right) \\ \Lambda_{c_2} = (1+2\delta)\Lambda_{c_1}/2 \end{cases} \tag{35}$$

and a solution $X = K/(1-k)$, $\Lambda = 0$ for the merged situation. Being proportional to X_{c_1}, X_{c_2} diverges in the same manner as $\delta \to 0$, and requires sign of K and δ to be the same, in order to lie in a physical range. It also diverges when $k \to 1$, as we have mentioned earlier, this is the case of a scattering of a neutral vortex pair on a vortex, which is out of the scope of the present paper. Finally we note, that since V_1 is proportional to the area of the vortex triangle A, the critical equilibrium position X_{c_2} corresponds to an aligned vortex configuration; in a similar manner we deduce that X_{c_1} corresponds to an equilateral configuration [20, 24].

A third possibility, when both $V_1 = 0$ and $V_2 = 0$, leads to the following system:

$$\begin{cases} \left(X-K\right)^2 - 4k^2Y = 0 \\ \left(K-(1-k)X\right)^2 - 4k^2Y = 0 \end{cases} \tag{36}$$

which yields:

$$\begin{cases} X_{c_3} = 2K/(2-k) \\ \Lambda_{c_3} = \left[K/\left(3+2\delta\right)\right]^{-2\delta}/4\ . \end{cases} \tag{37}$$

This critical case also corresponds to an aligned configuration, where the negative vortex of strength $-k$ is in the middle between the two identical

vortices. In near collapse situation $2 - k > 0$, and since X_{c_3} has to be positive, this critical situation appears only for positive total vortex angular momentum $K > 0$. Here a merged solution also exists ($X = 0,\ \Lambda = +\infty$), which corresponds to the merging of the two identical vortices. We also notice that the divergence of X_{c_3} for $k = 2$ corresponds to a special case of a neutral tripole, when the total vorticity is zero, and the center of vorticity is not defined.

Now we turn our attention to the three different specific cases distinguished by the sign of K. For each case, we will indicate which of the above found bifurcations do occur, and study the phase space trajectories of the effective Hamiltonian (22) for different regimes.

3.2 The case $K > 0$, $k \neq 1/2$

From the previous section, we know that the number of critical energies for this case depends on the sign of δ, i.e. whether $k > 1/2$ or $k < 1/2$. A special case $k = 1/2,\ \delta = 0$ will be treated separately. We start from the case $k < 1/2$, when all three critical cases (34), (35), (37) belong to the physical region. If we keep the value of k fixed, and vary the energy, we will encounter various motion regimes, separated by the three critical energies. To illustrate the critical situations we plotted the potential V as a function of X for the three different critical energies for $k = 0.2$ in Fig. 2. The critical energy Λ_{c_1} corresponds to the maximum possible value for which motion can exist; for $\Lambda = \Lambda_{c_2}$ an unstable equilibrium (saddle point) appears, and

motion becomes aperiodic; and in the last case of $\Lambda = \Lambda_{c_3}$, another saddle point appears right on the border of the physical region (corresponding to unstable aligned configuration).

Motions regimes for different energy ranges are listed below:

1. $\Lambda > \Lambda_{c_1}$ Motion impossible.

2. $\Lambda_{c_1} > \Lambda > \Lambda_{c_2}$ The potential has 2 zeros in the physical region, there exists a single type of periodic motion (see Fig. 3). When $\Lambda \to \Lambda_{c_2}$, the period diverges logarithmically $T(\Lambda) \sim 1/2 \ln|\Lambda - \Lambda_{c_2}|$ (see Fig. 5) due to proximity of a saddle-point; motion acquires typical near-separatrix character of relatively short velocity pulses separated by long stays in the saddle-point vicinity.

3. $\Lambda_{c_2} > \Lambda > \Lambda_{c_3}$ The potential has 4 zeros and two different types of periodic motion exist (see Fig. 4). Their period diverges as $T(\Lambda) \sim 1/4 \ln|\Lambda - \Lambda_{c_2}|$ when Λ approaches Λ_{c_2}, Fig. 5.

4. $\Lambda_{c_3} > \Lambda$ The potential has 4 zeros and two different types of periodic motion exist (see Fig. 6). As $\Lambda \to \Lambda_{c_3}$ (from both sides), the small-scale branch approaches a near-separatrix regime, its period diverges as $T(\Lambda) \sim \ln|\Lambda - \Lambda_{c_3}|$, for $\Lambda = \Lambda_{c_3}$ this branch becomes aperiodic.

For the case $k > 1/2$ only the critical value of X_{c_3} lies in the physical region, and only one regime of periodic motion exists (see Fig. 7).

3.3 The case $K < 0$, $k \neq 1/2$

When the total vortex angular momentum is negative, the critical root (37) lies outside the physical region, and therefore we expect less variety of motion types. Otherwise, this case is similar to the $K > 0$ case, in the sense that most phenomena described for $K > 0$ occur, but in a reverse order; for instance, when $k > 1/2$ we have three different regimes, which are analogue to the regimes of $K > 0$, $k < 1/2$ case. The different regimes, illustrated by their phase portraits, are listed below:

1. $\Lambda < \Lambda_{c_1}$ Motion impossible.

2. $\Lambda_{c_2} < \Lambda < \Lambda_{c_1}$ The potential has 2 zeros and a periodic motion is possible (see Fig. 8). In vicinity of a saddle point ($\Lambda \approx \Lambda_{c_2}$) motion period diverges in the same way as in $K > 0$ case.

3. $\Lambda_{c_2} < \Lambda$ The potential has 4 zeros and two different periodic motions are possible (see Fig. 9).

On the other hand the situation when $k < 1/2$, is analogous to the $K > 0$ and $k > 1/2$ situation. Namely, non of the critical values are physical, and we have only one type of periodic motion for all range of energies, see Fig. 10.

Now all the possible generic situations being described, we will proceed to the important singular cases $K = 0$ or $k = 1/2$.

3.4 The case $K = 0$.

In this situation any rescaling of length does not affect the value of K, and it is only the value of Λ that controls motion scales in the system. The expression for the effective potential $V(X)$ can be considerably simplified. It is convenient to introduce new variable

$$U = \frac{X^2}{4k^2 Y}, \tag{38}$$

then (21) becomes

$$V(U) = 8k^2 (1-k)^2 \left(U - \frac{1}{(1-k)^2} \right) (U-1) \ . \tag{39}$$

The zeros are simple and the different conditions imposed on X imply a motion confined between

$$1 \leq U \leq \frac{1}{(1-k)^2} \ , \tag{40}$$

In this situation double zero do not occur. Note that for exact collapse case, $k = 1/2$, transformation to new variable (38) is singular and does not work. In this case the potential $V(X)$ is constant; its value is negative only in a range of energies $\Lambda \in [1/2, 1]$, which means, that collapse configurations have their confined to this interval. We will return to the discussion of collapse configurations in section 4.

In this singular case, to visualize the approach to collapse ($k \to 1/2$),

it is better to have k fluctuating and Λ fixed. This is due to the fact that, when $k = 1/2$, which corresponds to the merging conditions, the motion is possible only within a range of energies $\Lambda_2 > \Lambda > \Lambda_1$. The phase portrait of trajectories taken for different values of k is shown in Fig. 11 and Fig. 12. These two figures are taken close to the values $\Lambda = 1/2$ and $\Lambda = 1$; we notice for the $k = 1/2$ case two straight lines corresponding to the two possible motions of expansion or collapse. Note, that when $\Lambda \notin [1/2\,,\ 1]$ a collapse cannot occur, which means that the trajectories for $k < 1/2$ and $k > 1/2$ are similar to those shown in Fig. 11, but do not intersect on the top view.

3.5 The case $k = 1/2$

This special case corresponds to "scale invariance", meaning that any length can be rescaled without changing the energy of the system. Therefore the energies of the critical situations should not depend on the value of K, which is scale dependent. The effective potential is now simply a fraction of polynomial and can be rewritten as

$$V(X) = \lambda\,(X - X_1)\,(X - X_2)\,(X - X_3)\,(X - X_4)\,/X^4\,, \tag{41}$$

where

$$X_1 = \frac{K}{1/2 - \Lambda}\,,\ X_2 = \frac{K}{1/2 + \Lambda}\,,\ X_3 = \frac{K}{1 - \Lambda}\,,\ X_4 = \frac{K}{1 + \Lambda}\,, \tag{42}$$

and

$$\lambda = \frac{2(1/2+\Lambda)(1/2-\Lambda)(1+\Lambda)(1-\Lambda)}{2\Lambda^2}\,. \tag{43}$$

We have three critical values, the first two $\Lambda_{c_1} = 1$ and $\Lambda_{c_2} = 1/2$ correspond to the divergence of one root, while the third $\Lambda_{c_3} = 1/4$ corresponds to a double root situation $X_2 = X_3$. Depending on the sign of K we have the following allowed supports:

1. $K > 0$ and $\Lambda < \Lambda_{c_3}$ implies $X_1 > X > X_2$. The potential $V(X)$ for the critical situation $\Lambda = 1/4$ is illustrated on Fig. 13. As we approach collapse ($K \to 0$) this motion vanishes.

2. $K > 0$ and $\Lambda_{c_3} < \Lambda < \Lambda_{c_2}$ implies $X_1 > X > X_3$. The potential $V(X)$ for the critical situation $\Lambda = 1/2$ is illustrated on Fig. 14. As we approach collapse ($K \to 0$) this motion also vanishes. Nevertheless this case is interesting as an aperiodic motion very close to collapse is reached as $\Lambda \to 1/2$. The period of the motion as a function of $|\Lambda - 1/2|$ is shown in Fig. 15. It diverges according to a power law:

$$T \sim (\Lambda - 1/2)^{-3/2}\ , \tag{44}$$

   (see the Appendix for its derivation). Phase space portraits of the trajectories are illustrated in Fig. 16.

3. $K > 0$ and $\Lambda_{c_2} < \Lambda < \Lambda_{c_1}$, then $X > X_3$. This motion is the closest to the collapse, as infinite expansion is possible, but X is bounded from

below. In this situation we may see a collapse course, which rebounds on X_3 and goes for an infinite expansion. As we approach collapse ($K \to 0$) $X_3 \to 0$, and depending on the sign of $\dot{X}$ a full collapse can occur.

4. $K > 0$, $\Lambda_{c_1} < \Lambda$ and $K < 0$, $\Lambda < \Lambda_{c_2}$ motion impossible.

5. $K < 0$ and $\Lambda_{c_2} < \Lambda < \Lambda_{c_1}$, then $X > X_1$. We have a similar situation as the one discussed for the $K > 0$ and $\Lambda_{c_2} < \Lambda < \Lambda_{c_1}$.

6. $K < 0$ and $\Lambda_{c_1} < \Lambda$, then $X_3 > X > X_1$. Here we can anticipate a similar situation as the one discussed for the $K > 0$ and $\Lambda_{c_3} < \Lambda < \Lambda_{c_2}$.

4 Collapse scenarii

As we have mentioned earlier, for the collapse to happen, two "resonance conditions" have to be satisfied. First, the sum of the vortex strengths inverses have to be zero. This condition does not impose any geometrical restrictions on vortex positions, for a given system of vortices it is either satisfied or not. Initial positions leading to collapse are specified by the second collapse condition, $K = 0$. It also defines the range of energies, for which the self-similar dynamics can occur (for $k = 1/2$), but does not tell in which direction (collapse or expansion) it will go.

For a given vortex configuration, let us consider a coordinate system with x-axis passing through the two positive vortices ($k_1 = k_2 = 1$) and an

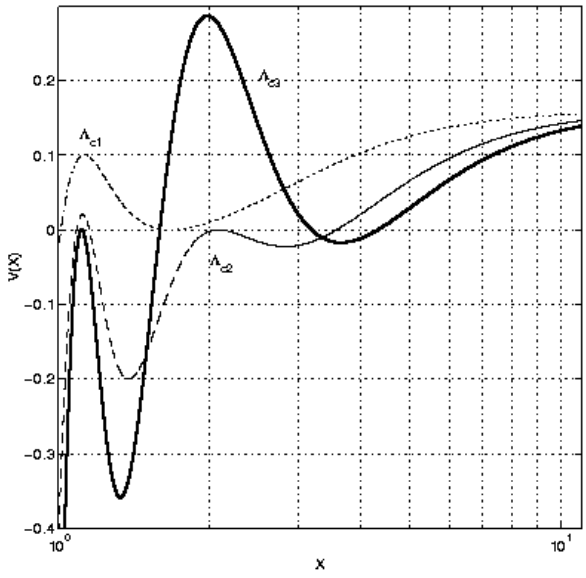

Figure 2: The potential $V(X)$ for the three critical cases. $k = 0.2$. For $\Lambda = \Lambda_{c_1}$ the motion appears, for $\Lambda = \Lambda_{c_2}$ two motions are possible, and for $\Lambda = \Lambda_{c_3}$ an unstable aligned configuration is approached as $X \to X_{c_3}^+$.

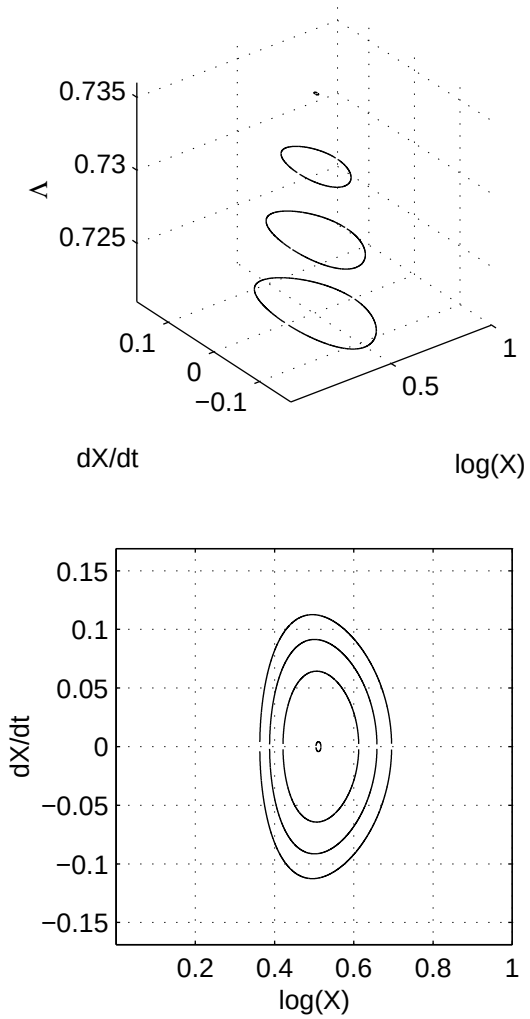

Figure 3: Phase space portrait close to Λ_{c_1} for different energies for the case $K = 1$ and $k = 0.2$. The bottom figure is the top view of the upper one. Once the first critical situation is reached a motion is possible.

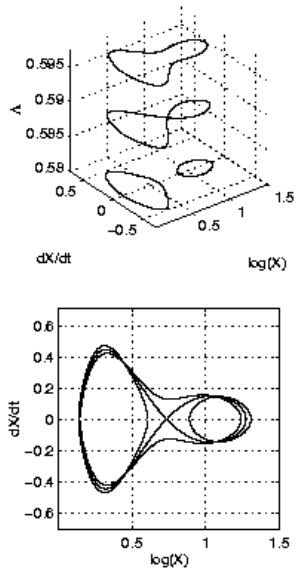

Figure 4: Phase space portrait close to Λ_{c_2} for different energies for the case $K = 1$ and $k = 0.2$. The bottom figure is the top view of the upper one. Once the second critical situation is reached, the single possible trajectory reaches the separatrix, and the splitting in two possible motions occurs.

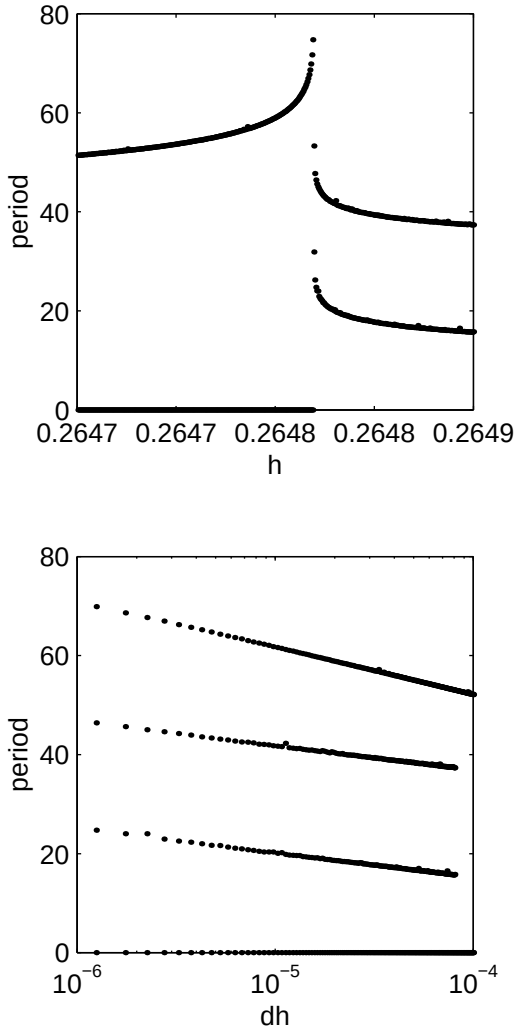

Figure 5: Period of the motion versus energy ($dh = |H(X) - H_{c_2}|$) for $k = 0.2$ close to $\Lambda = \Lambda_{c_2}$. We notice the logarithmic behavior of the divergence, we note also that the sum of the slopes of the two right branches (lower) is equal to the slope of the left branch (upper).

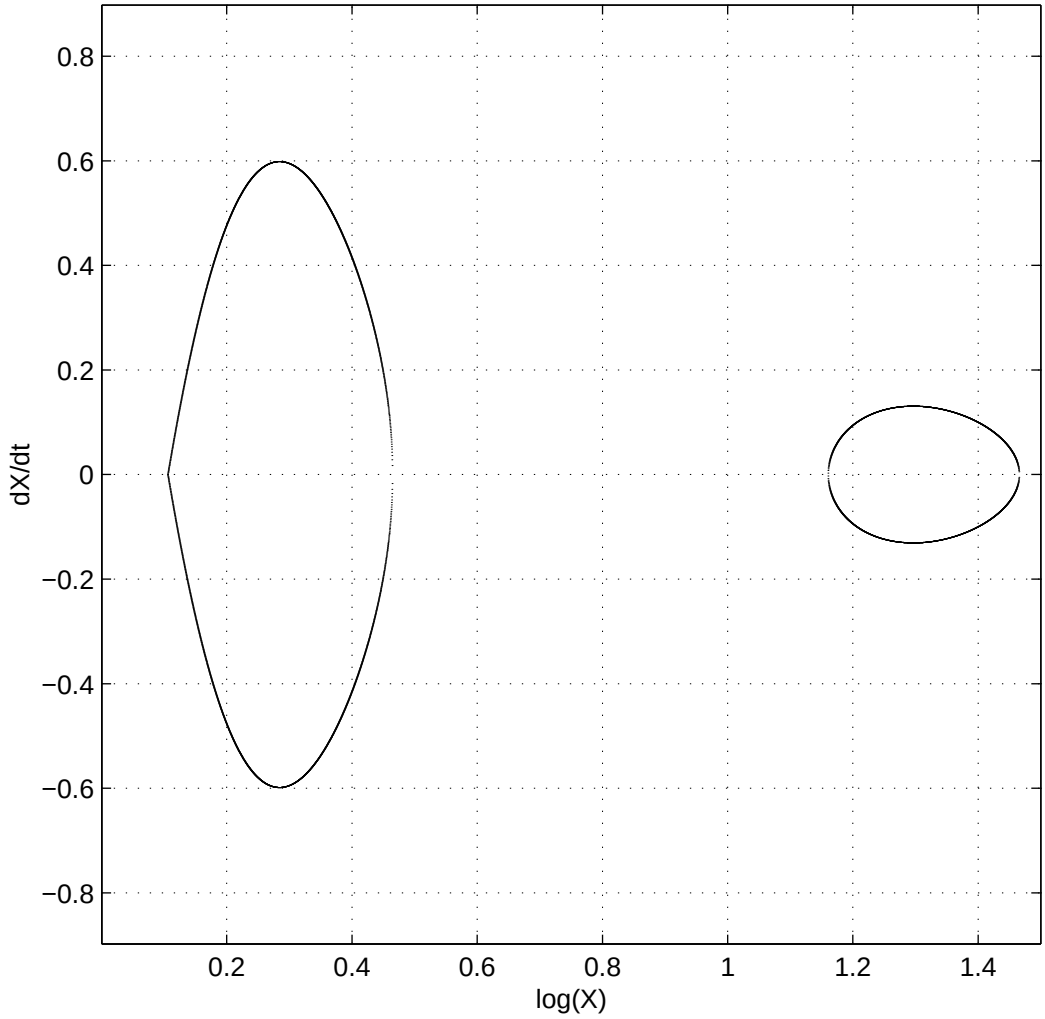

Figure 6: Phase space portrait for $\Lambda = \Lambda_{c_3}$ for the case $K = 1$ and $k = 0.2$. A splitting occurs like for $\Lambda = \Lambda_{c_2}$ but the triangle conditions prevent the existence of a third branch. We notice the sharp angle at $X = X_{c_3}$.

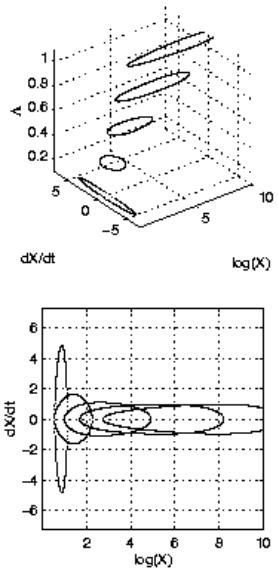

Figure 7: Phase space portrait for different values of Λ in the case $K = 1$ and $k = 0.55$. The bottom figure is the top view of the upper one. The motion remains periodic. As Λ increases, we notice the growth of the range of length scales explored by the motion.

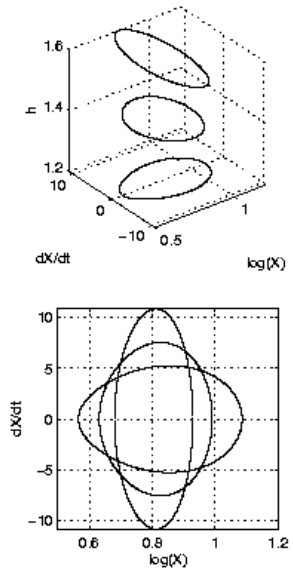

Figure 8: Phase space portrait close to Λ_{c_1} for different values of Λ in the case $K = -1$ and $k = 0.55$. The bottom figure is the top view of the upper one. Once the first critical situation is reached a motion is possible.

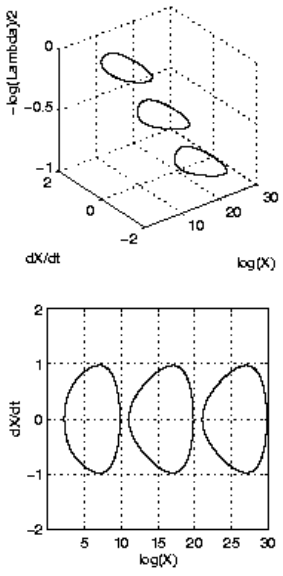

Figure 9: Phase space portrait close to Λ_{c_2} for different values of Λ in the case $K = -1$ and $k = 0.55$. The bottom figure is the top view of the upper one. Once the second critical situation is reached, the single possible trajectory reaches the separatrix, and the splitting in two possible motions occurs.

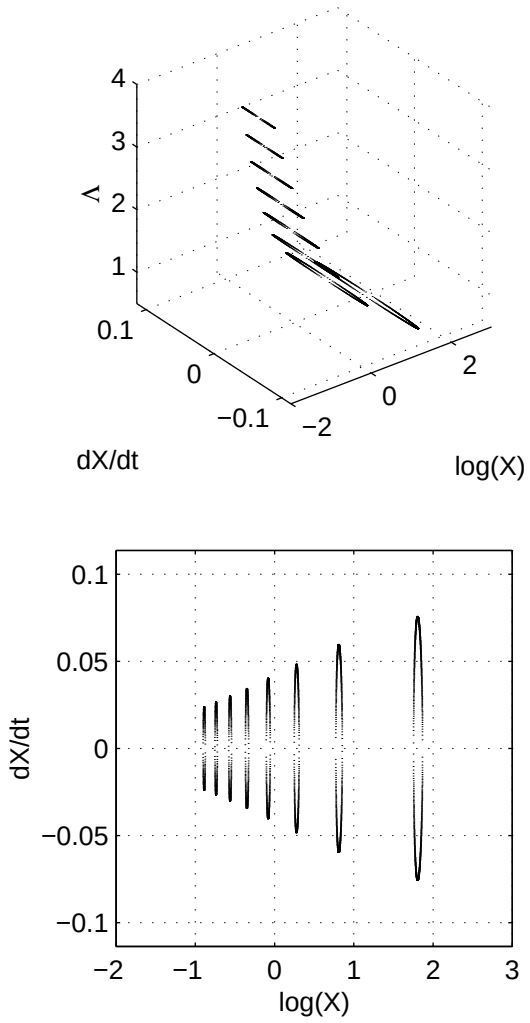

Figure 10: Phase space portrait for different values of Λ in the case $K = -1$ and $k = 0.2$. The bottom figure is the top view of the upper one. The value of Λ determines the typical length scale of the periodic motion (the value of K is fixed).

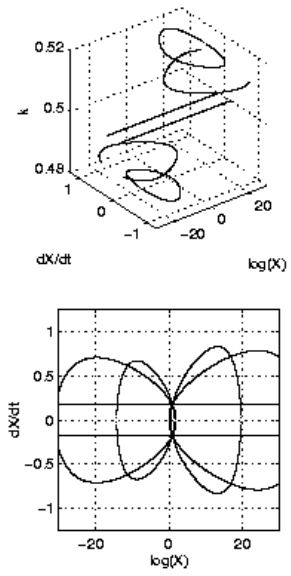

Figure 11: Phase space portrait close to Λ_{c_2} for different values of k in the case $K = 0$. The bottom figure is the top view of the upper one.For this singular case we notice the two lines at $k = 1/2$ corresponding one to collapse and one to infinite expansion. On the projection plot (bottom), the trajectories $k < 1/2$ and $k > 1/2$ seem to intersect on those two lines. For $\Lambda < \Lambda_{c_2}$ collapse is not possible, and the trajectories do not intersect. We notice that close to the collapse condition $k = 1/2$, the values $k < 1/2$ describe a collapse motion, while $k > 1/2$ describes the expansion motion.

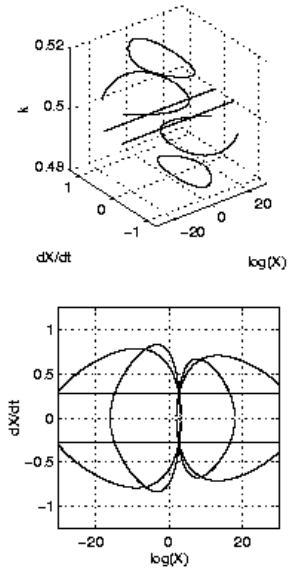

Figure 12: Phase space portrait close to Λ_{c_1} for different values of k for the case $K = 0$. The bottom figure is the top view of the upper one.For this singular case we notice the two lines at $k = 1/2$ corresponding one to collapse and one to infinite expansion. On the projection plot (bottom), the trajectories $k < 1/2$ and $k > 1/2$ seem to intersect on those two lines. For $\Lambda > \Lambda_{c_1}$ collapse is not possible, and the trajectories do not intersect. We notice that close to the collapse condition $k = 1/2$, the values $k < 1/2$ describe a collapse motion, while $k > 1/2$ describes the expansion motion.

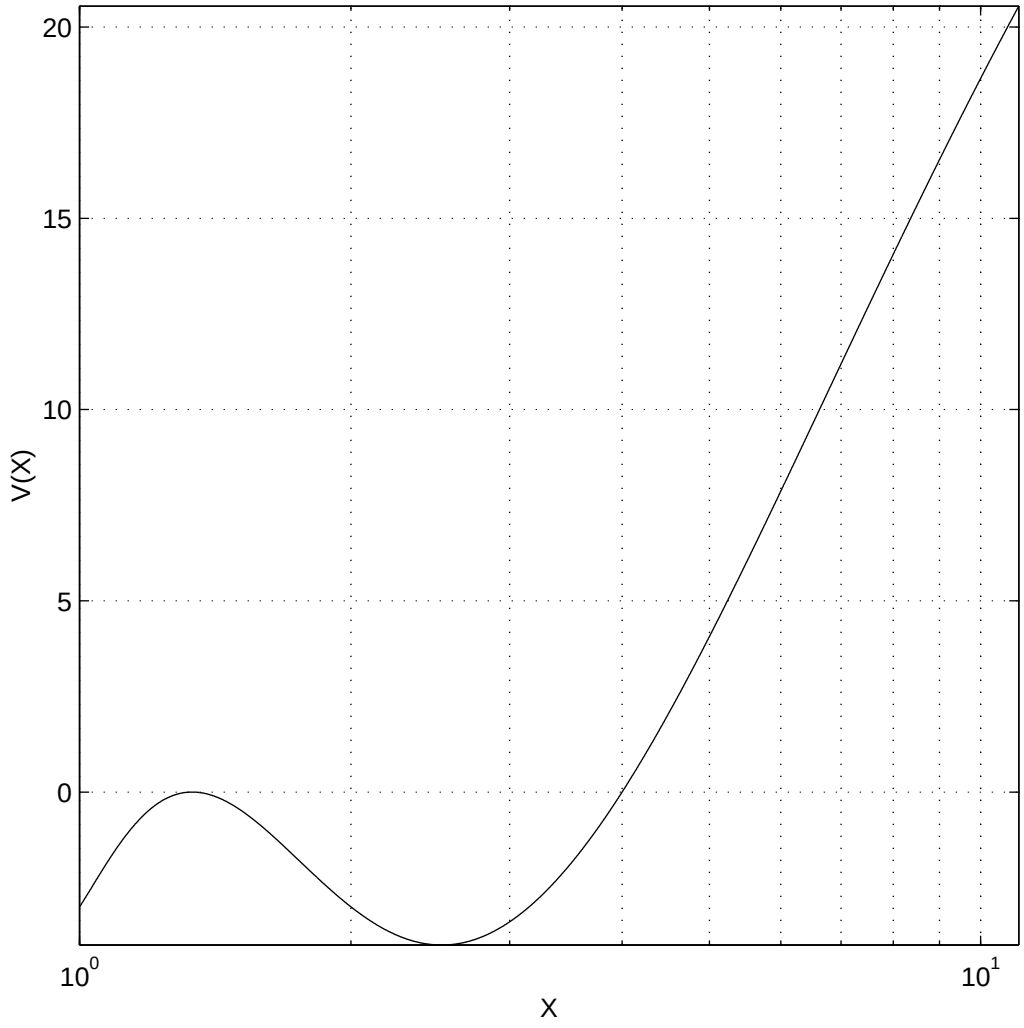

Figure 13: The effective potential $V(X)$ in the singular case $k = 1/2$ ($\delta = 0$) for the critical energy corresponding to $\Lambda = 1/4$: the double root case.

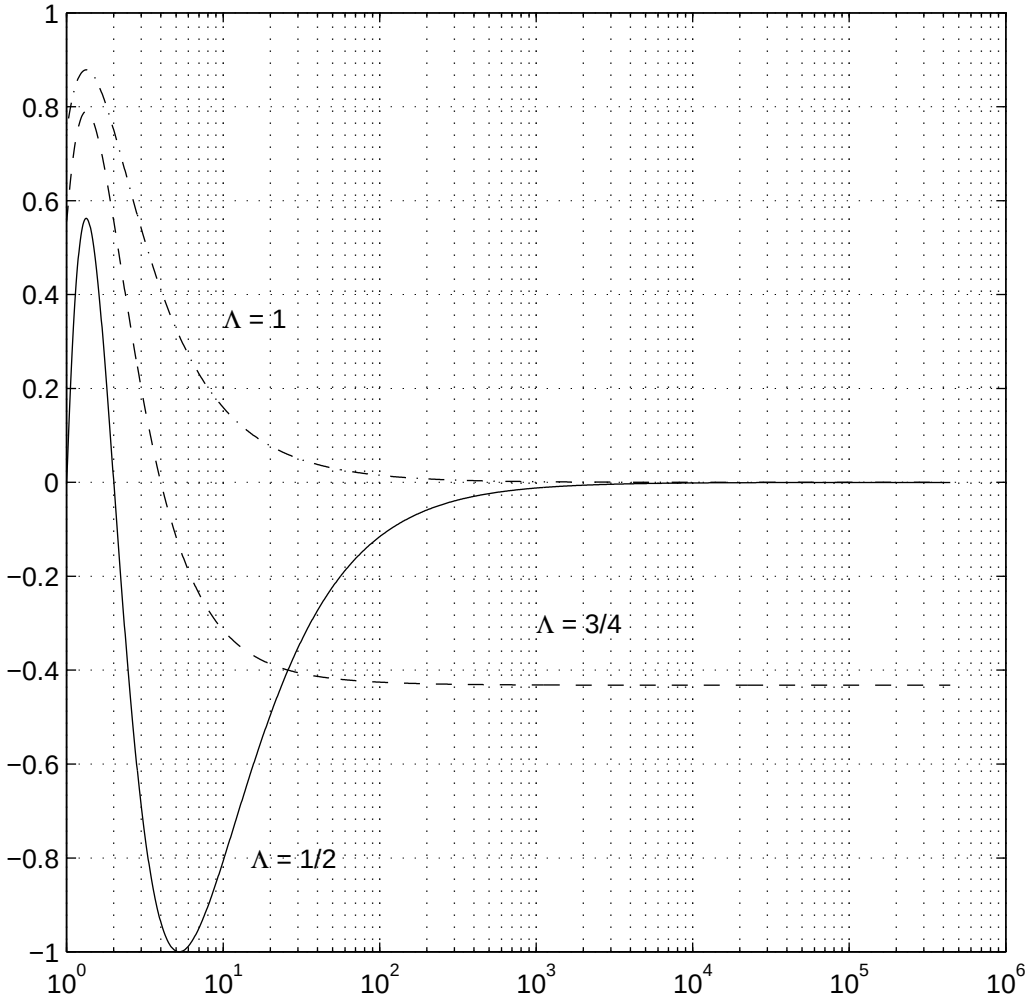

Figure 14: Evolution of the effective potential $V(X)$ in the singular case $k = 1/2$ ($\delta = 0$) within the energy range corresponding to possible collapse $\Lambda \in [1/2, 1]$. We notice that unbounded motion occurs.

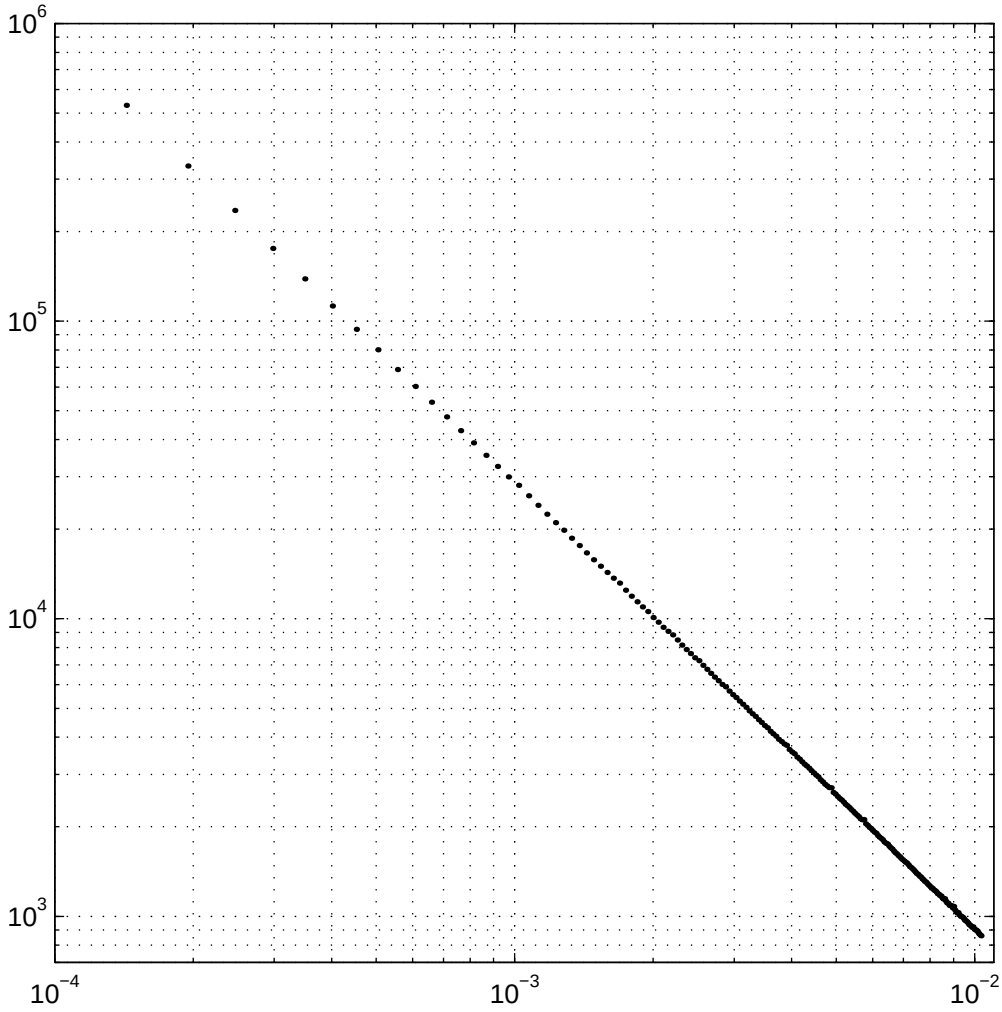

Figure 15: Period of the periodic motion ($\Lambda < 1/2$) motion versus $|\Lambda - 1/2|$ in the singular case $k = 1/2$ ($\delta = 0$). We notice a power-law divergence of the period as we approach collapse. The measured exponent is 3/2. See appendix A for the analytical computation.

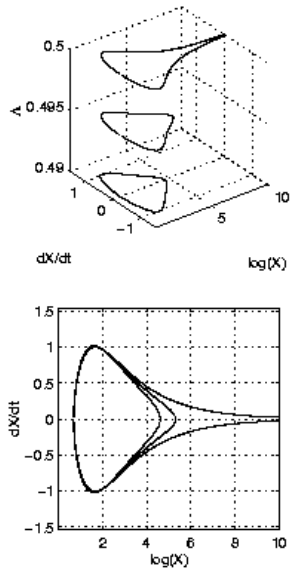

Figure 16: Phase space portrait for different values of Λ close to $\Lambda_c = 1/2$, in the case $K = 1$ and $k = 1/2$ ($\delta = 0$). The bottom figure is the top view of the upper one. We notice the singular evolution of the motion to larger scales as Λ approaches Λ_c.

origin in the middle between them, so that positive vortices have coordinates $(-d/2, 0)$ and $(d/2, 0)$, where d is the distance between them. Denoting the coordinates of the third vortex by (x, y) we can rewrite the condition $K = 0$ as

$$x^2 + y^2 = \frac{d^2}{2k}(1 - k/2) \tag{45}$$

i.e. third vortex has to lie on a "critical circle" centered at the midpoint between the two positive ones, with a radius $(d/2)\sqrt{2/k - 1}$.

In the "resonant" case $k = 1/2$, the critical circle represents a set of initial conditions leading to a self-similar collapse or expansion. Level lines of Λ cross the circle in four points for $\Lambda \in [1/2; 1]$, see Figure 17. These points are reflections of each other in the coordinate axes, this symmetry leads the coordinate axis to divide the plane in four dynamically equivalent quadrants. A reflection of a vortex configuration is equivalent to changing the direction of time, so that points in adjacent quadrants have opposite directions of their dynamics. From the original equations (8), we deduce, that the parts of the critical circle lying in the I and III quadrants lead to a finite-time collapse, and those in II and IV quadrants to an infinite self-similar expansion.

Four intersections of the critical circle with the coordinate axes are equilibrium positions, where Λ reaches its limiting values (on the circle); the maximum value $\Lambda = 1$ corresponds to the equilateral triangle, and the minimum $\Lambda = 1/2$ to collinear configuration.

We define a *rate of collapse* as a rate of change of the squared distance

between the two positive vortices, i.e. as $\dot{X}$. In this case, self-similar motion will have constant rate of collapse. Indeed, vortex velocities are inversely proportional to the inter-vortex distances, so that $\dot{X} = 2R_1\dot{R}_1$ is independent of the scale of the motion. The rate of collapse is determined by the vortex energy:

$$\dot{X}(\Lambda) = \sqrt{4(1-\Lambda^2)(1/4-\Lambda^2)}, \tag{46}$$

it tends to zero when Λ approaches one of the equilibrium values $\Lambda = 1/2, 1$.

In general, approaching collapse means taking the limits $K \to 0$ and $k \to 0.5$. These limits are not commutative, and for certain situations, the result depends on how the limits are taken, e.g. these limits may induce the divergence of $X_{c_{1,2}}$ or set them to zero or any value. Therefore a three vortex system can approach collapse in a number of different ways. For instance, if we take one limit after another, we can obtain the properties of the motion from the cases listed in §3.4 and §3.5. It is also interesting to study some of the scenarios, when the limits $K \to 0^{+-}$ and $k \to 0.5^{+-}$ are taken simultaneously, leading to an interplay of different situations, described in the previous section. As an example, consider a limit $K \to 0^+$, $k \to 0.5^-$ taken along the line $K/\delta = C$, where C is a constant. In this case, the saddle-point critical values $(X_{c_2}, \Lambda_{c_2}$ tend to $(C, 1/2)$, i.e. the scale of the inner potential well (bounded by X_{c_2}) stay the same. At the same time the outer potential well spreads to infinity (see Fig 4 and Fig. 11), and we have a situation, when two types of motion, corresponding to the same value of

vortex energy, have entirely different length scales.

5 Tracer advection near collapse

As we have mentioned, a prominent feature of near collapse dynamics is a generation of new length scales, which can differ from the length scale of the original configuration by orders of magnitude (see for instance (44)). This property has a strong influence on the mixing properties of the vortex flow. As an illustration, we compare the motion of passive particles (tracers) in a velocity field of a near collapse configuration, with that in a typical "far from collapse" flow. A stream function of the flow, induced by moving vortices can be written as:

$$\psi(\mathbf{x},t) = -\frac{1}{2\pi}\sum_{i=1}^{3}\ln|\mathbf{x}-\mathbf{x}_i(t)| \tag{47}$$

corresponding equations of tracer motion are:

$$\frac{d\mathbf{r}(t)}{dt} = \mathbf{e}_z \wedge \nabla\psi \tag{48}$$

where $\mathbf{r}(t)$ denotes tracer position vector. Vortex trajectories $\mathbf{x}_i(t)$ are periodic in a corotating reference frame, where (48) have a structure of a Hamiltonian system with 11/2 degrees of freedom [17, 29], so in a generic three-vortex flow some of the tracer trajectories are regular, and some are chaotic. To visualize advection patterns, we numerically construct Poincare section of tracer trajectories (in a corotating frame), which is an expedient tool for estimation

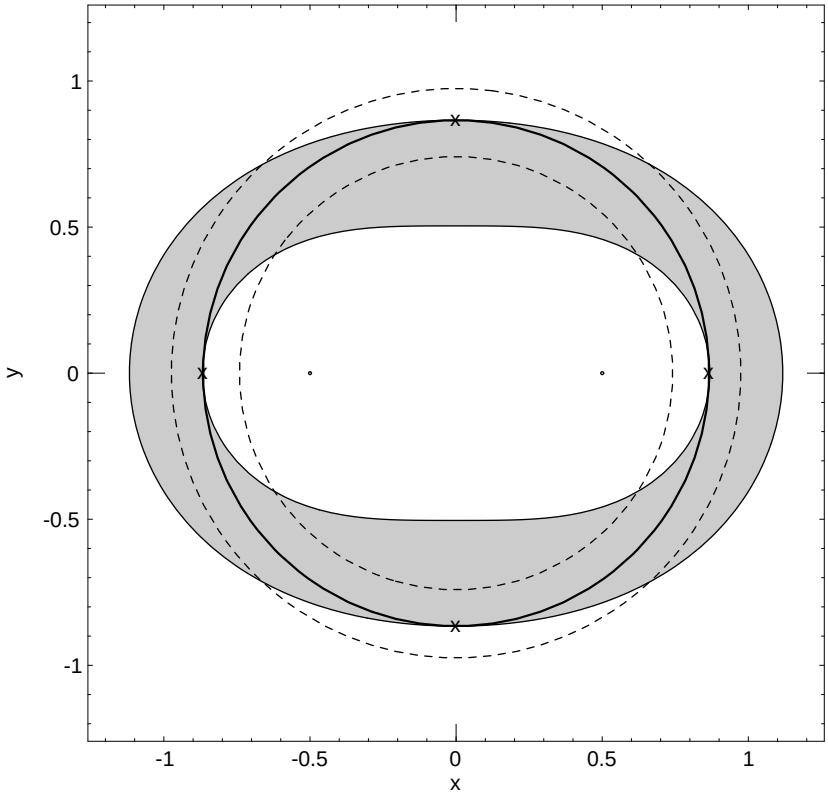

Figure 17: The approach to collapse. Initial positions available for the vortex with negative strength. The two vortex with strength 1 are fixed, and located by the two thick points on the plot. Circles refer to different values of the constant K, while the oval curves correspond to different values of Λ. The shaded region correponds to initial conditions leading to the aperiodic infinite expansion type of motion.

of the degree of chaotization of advection, location of the main structures in the chaotic regions, etc. In Fig. 18, an example of an advection pattern of a far from collapse flow is presented. A large connected mixing region, regular cores around vortices, elliptic islands are typical elements of a tracer phase space in three-vortex flows [17, 29]. Two most important length scales in the advection pattern, associated with its robust features, are the outer radius of the mixing region and the radii of vortex cores. Generally, these two scales are comparable (their ratio is about one order of magnitude or less). However in advection patterns of near collapse vortex configurations, these length scales become considerably different, as the core radii tend to zero when approaching collapse see Fig. 19. The figures Fig. 18 and Fig. 19 are showed to emphasize that tracers chaotic dynamics in the near collapse case, is different than the dynamics without collapse. A more detailed analysis will be described in another article.

6 Conclusion

The behavior of a three point vortex system in a near collapse state, studied in this paper, shows a number of nontrivial dynamical features, that may play an important role in studies of more general two-dimensional flows. In particular, a possibility of vorticity concentration allows one to speculate on the fact that the collapse situation exhibits some basics mechanisms which could trigger $2D$ turbulence, and in the same spirit, raise the question whether or

not the statistics made out of the Grand Canonical Ensemble are physically relevant. The study of vortex motion near the critical situations, has also revealed itself interesting in exhibiting non-generic power-law growth of the period in §3.5. The scale invariance property of the collapse configurations, implies the possibility of new length scale generation. In the vicinity of the degenerate cases observed in §3.2 and §3.3, a small perturbation, for instance a sound wave, or corrections to the vortex Hamiltonian due to finite vortex size, would allow to jump from one motion type to the other. Since the two motion types correspond to very different length scales, these jumps could be associated with vortex collapse or vortex splitting.

Another consequence of the peculiar character of near collapse dynamics concerns properties of passive particle advection in the flows generated by such systems. In this paper we limit ourselves to a short illustration of how the approach to collapse influences a degree of tracer mixing; a more detailed study of this topic will be presented elsewhere. For instance, it is interesting, how the scale invariance of the Hamiltonian in case $\delta = 0$, affects tracer phase space topology, which is then defined solely by the value of K. To conclude, we emphasize once again the fact, that near collapse dynamics comprises several types of motion. Their time and length scales differ considerably, depending on the way the collapse conditions are violated, which makes a problem of an effect of small perturbations on self-similar contracting (unstable) spiral motion very interesting.

A Power-law divergence

From the effective Hamiltonian (22) the period of the motion in the case $k = 1/2$ and for instance $K > 0$ and $\Lambda < 1/2$ (see Fig. 15) is then simply defined by

$$T = 2 \int_{X_3}^{X_1} \frac{dX}{\sqrt{-V(X)}} \,, \tag{49}$$

where X_1 and X_3 are defined in (42). To obtain the asymptotic expression of the period as $\Lambda \to 1/2^-$, we use some simple equivalents, and write

$$T \sim 2\lambda^{-1/2} \int_1^{X_1} \frac{dX}{\sqrt{X_1/X - 1}} \sim 4\lambda^{-1/2} X_1 \,, \tag{50}$$

using the expression (42) for X_1 and (43) for λ, we obtain the asymptotic behavior of the period as a function of Λ and K

$$T \sim K\sqrt{\frac{3}{2}} \left(\frac{1}{2} - \Lambda\right)^{-3/2} \,. \tag{51}$$

The period diverges as $(1/2 - \Lambda)^-3/2$ when Λ approaches the collapse value of $1/2$, and $K \neq 0$.

Acknowledgments

This work was supported by the US Department of Navy, Grant No. N00014-96-1-0055, and the US Department of Energy, Grant No. DE-FG02-92ER54184.

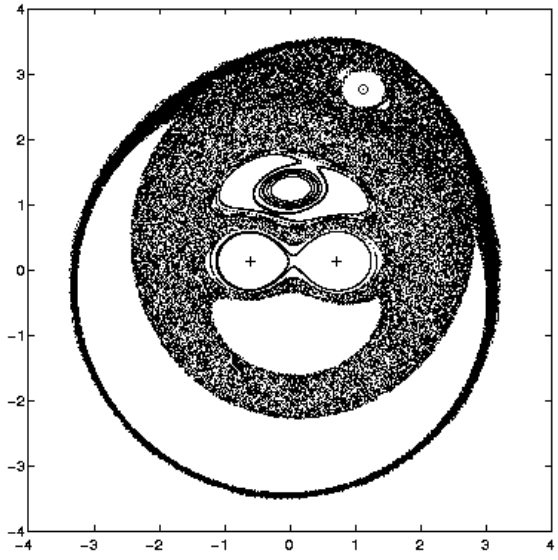

Figure 18: Far from collapse $\delta = 0.4$. Poincare section of 253 passive tracers in the flow field generated by three point vortex. The run is over 4000 periods. The constant of motions are $\Lambda = 0.9$, $K = 0$. The vortex strengths are $(-0.1,\ 1,\ 1)$. The period of the motion is $T = 6.59$.

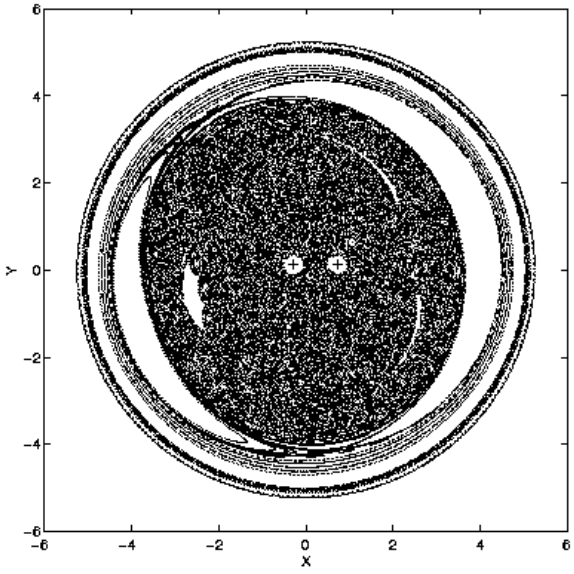

Figure 19: Far from collapse $\delta = 0.09$. Poincare section of 253 passive tracers in the flow field generated by three point vortex. The run is over 4000 periods. The constant of motions are $\Lambda = 0.9$, $K = 0$. The vortex strengths are $(-0.41,\ 1,\ 1)$. The period of the motion is $T = 36.86$.

References

[1] P. Tabeling, A.E. Hansen, J. Paret, *Forced and Decaying 2D turbulence: Experimental Study*, in "Chaos, Kinetics and Nonlinear Dynamics in Fluids and Plasmas", eds. Sadruddin Benkadda and George Zaslavsky, p. 145, (Springer 1998)

[2] R. Benzi, G. Paladin, S. Patarnello, P. Santangelo and A. Vulpiani, *Intermittency and coherent structures in two-dimensional turbulence*, J. Phys A **19**, 3771 (1986)

[3] R. Benzi, S. Patarnello and P. Santangelo, *Self-similar coherent structures in two-dimensional decaying turbulence*, J. Phys A **21**, 1221 (1988)

[4] J. B. Weiss, J.C. McWilliams, *Temporal scaling behavior of decaying two-dimensional turbulence*, Phys. Fluids A **5**, 608 (1992)

[5] J.C. McWilliams, *The emergence of isolated coherent vortices in turbulent flow*, J. Fluid Mech. **146**, 21 (1984)

[6] J.C. McWilliams, *The vortices of two-dimensional turbulence*, J. Fluid Mech. **219**, 361 (1990)

[7] D. Elhmaïdi, A. Provenzale and A. Babiano, *Elementary topology of two-dimensional turbulence from a Lagrangian viewpoint and single particle dispersion*, J. Fluid Mech. **257**, 533 (1993)

[8] G. F. Carnevale, J.C. McWilliams, Y. Pomeau, J. B. Weiss and W. R. Young, *Evolution of Vortex Statistics in Two-Dimensional Turbulence*, Phys. Rev. Lett. **66**, 2735 (1991)

[9] N. J. Zabusky, J.C. McWilliams, *A modulated point-vortex model for geostrophic, β-plane dynamics*, Phys. Fluids **25**, 2175 (1982)

[10] P.W.C. Vobseek, J.H.G.M. van Geffen,, V.V. Meleshko, G.J.F. van Heijst, *Collapse interaction of finite-sized two-dimensional vortices*, Phys. Fluids **9**, 3315 (1997)

[11] O.U. Velasco Fuentes, G.J.F. van Heijst, N.P.M. van Lipzig, *Unsteady behaviour of a topography-modulated tripole*, J. Fluid Mech. **307**, 11 (1996)

[12] J. B. Weiss, A. Provenzale, J.C. McWilliams, *Lagrangian dynamics in high-dimensional point-vortex systems*, Phys. Fluids **10**, 1929 (1998)

[13] I.A. Min, I. Mezic, A. Leonard, *Levy stable distributions for velocity difference in systems of vortex elements*, Phys. Fluids **8**, 1169 (1996)

[14] V.V. Melezhko, M.Yu. Konstantinov, A.A. Gurzhi and T.P. Konovaljuk, *Advection of a vortex pair atmosphere in a velocity field of point vortices*, Phys. Fluids A **4**, 2779 (1992)

[15] A. Babiano, G. Boffetta, A. Provenzale and A. Vulpiani, *Chaotic advection in point vortex models and two-dimensional turbulence*, Phys. Fluids **6**, 2465 (1994)

[16] L. Zannetti and P. Franzese, *Advection by a point vortex in a closed domain*, Eur. J. Mech., B/Fluids **12**, 43 (1993)

[17] Z. Neufeld and T. Tél, *The vortex dynamics analogue of the restricted three-body problem: advection in the field of three identical point vortices*, J. Phys. A: Math. Gen. **30**, 2263 (1997)

[18] Z. Neufeld and T. Tél, *Advection in chaotically time-dependent flow*, Phys. Rev E **57**, 2832 (1998)

[19] G. Boffetta, A. Celani and P. Franzese, *Trapping of passive tracers in a point vortex system*, J. Phys. A: Math. Gen. **29**, 3749 (1996)

[20] H.Aref, *Motion of three vortices*, Phys. Fluids **22**, 393 (1979)

[21] D. G. Dritschel, N. J. Zabusky, *On the nature of the vortex interactions and models in unforced nearly-inviscid two-dimensional turbulence*, Phys. Fluids **8**(5), 1252 (1996)

[22] E.A. Novikov, Yu.B. Sedov, *Vortex collapse*, Sov. Phys. JETP **22**, 297 (1979)

[23] J.L. Synge, *On the motion of three vortices*, Can. J. Math. **1**, 257 (1949)

[24] J. Tavantzis and L. Ting, *The dynamics of three vortices revisited*, Phys. Fluids **31**, 1392 (1988)

[25] Y. Kimura, *Parametric motion of complex-time singularity toward real collapse*, Physica D **46**, 439 (1990)

[26] C. Machioro and M. Pulvirenti, *Mathematical theory of uncompressible nonviscous fluids*, Applied Mathematical Science 96 (Springer-Verlag, New York, 1994)

[27] P. Saffman, *Vortex Dynamics*, Cambridge Monographs on Mechanics and Applied Mathematics (Cambridge University Press, Cambridge, 1995)

[28] H.Aref, *Integrable, chaotic and turbulent vortex motion in two-dimensional flows*, Ann. Rev. Fluid Mech. **15**, 345 (1983)

[29] L. Kuznetsov and G.M. Zaslavsky. *Regular and Chaotic advection in the flow field of a three-vortex system.* Phys. Rev E **58**, 7330 (1998)